Porous piezoelectric materials for energy harvesting

G. Martinez-Ayuso[1], **M. I. Friswell**[1], **S. Adhikari**[1], **H. Haddad Khodaparast**[1], **C. A. Featherston**[2]
[1] Swansea University, Bay Campus
Fabian Way, Crymlyn Burrows, Swansea SA1 8EN, Wales, United Kingdom
e-mail: **841238@swansea.ac.uk**

[2] Cardiff University, School of Engineering,
Queen's Buildings, The Parade, Cardiff CF24 3AA, Wales, United Kingdom

Abstract
In this paper, we assess the energy harvesting capabilities of porous piezoelectric material under harmonic excitation and investigate the advantages of functionally grading the air inclusions. A cantilever beam energy harvester with base excitation is used to demonstrate the effects of porosity on the power generated. A homogenization step using the analytical Mori-Tanaka approach is performed initially to reduce the computational requirements. This homogenization will estimate the material properties for different levels of porosity. An Euler-Bernoulli beam model is used to efficiently estimate the power generated for a piezoelectric sensor with uniform properties. A 2D finite element model is then developed to verify the beam model; this detailed model may be used to analyze harvesters where the porosity varies through the thickness or along the length of the beams. An optimization is performed, focusing on the impact of the percentage of inclusions on the energy harvesting efficiency.

1 Introduction

Piezoelectric materials generate an electrical field when a strain is applied to them, which is called the direct piezoelectric effect. These materials also exhibit the opposite effect, where a strain arises when an electrical field is applied, and this is called inverse piezoelectric effect. These materials are widely used in many applications, for example inkjet printers, sonars, heart monitors, tennis racquets, hydrophones or air bag sensors, either as actuators (direct effect) or as sensors (inverse effect). A more recent application is energy harvesters using a vibration source, that are used to power small devices or recharge batteries. A. Ertuk and D.J. Inman [1–3] studied piezoelectric cantilever bimorph beams for energy harvesting, both theoretically and experimentally. A. Sodano [4–6] gave an extensive reviews of the applications of piezoelectric materials to energy harvesting. M.I. Friswell and S. Adhikari explored the possibilities of piezoelectric devices to harvest energy from non-linear vibration [7] and from broadband excitation [8].

For energy harvesting applications, two coefficients are used to measure the capability of a piezoelectric energy harvester; the electromechanical coupling and the capacitance [2]. These two coefficients depend on the material properties and the device geometry. The electromechanical coupling coefficient measures the capability of the harvester to convert strain to electrical field, and hence is based on the stiffness and piezoelectrical properties of the materials. Most approaches have focused on maximizing the strain in the piezoelectrical material through a careful optimization of the geometry [9, 10]. Some researchers have studied the impact of the electrical circuit configuration on the power output [11, 12], but few researchers have focused on reducing the capacitance. The capacitance depends on the dielectric characteristics of the material and the geometry of the device. The dielectric coefficients may be reduced by mixing the

piezoelectric material with other materials which lower permittivity to create new composite materials. A significant reduction for porous piezoelectric material with inclusions of air, which has very low dielectric properties was reported in [13]. Porous piezoelectric materials have been studied by a number of authors. J.F. Li et al. [14] studied this material experimentally for actuator applications. E. Roncari et al. [15] and J. I. Roscow et al. [16] reviewed the manufacturing process of porous piezoelectric materials. M.L. Dunn and M. Taya[17] applied homogenization mean field theory to analytically predict the mechanical, piezoelectric and dielectric properties of porous piezoelectric materials.

There is little understanding of the effects of porous piezoelectric materials in energy harvesting. This paper aims to fill this gap in knowledge through a study of porous piezoelectric bimorph beams under harmonic excitation. Using the mean-field homogenization approach, the effective material properties are calculated for different percentage of porosity. These properties are then used to model a piezoelectric cantilever beam harvester under harmonic base excitation, which drives a load resistor. The voltage and power are calculated for various levels of porosity, different excitation frequencies and different load resitance values.

The structure of this paper is summarized as follows. In section 2 the modeling approach is described; this section is divided into three parts, according to the different methods used. Section 2.1 introduces the Mori-Tanaka method to homogenize composite materials such as the porous piezoelectric material. Section 2.2 gives the analytical solution for a bimorph beam based on Euler-Bernoulli beam theory. Finally, a finite element model (FEM) is used to verify the beam model in section 2.3; this model will enable functionally graded piezoelectric material to be analyzed and optimized. The results for an example harvester device are given in section 3 and the main conclusions are summarized in section 4.

2 Modelling of a cantilever beam energy harvester

The constitutive equations for linear piezoelectricity can be derived by considering an electric enthalpy function $\mathcal{H}$ defined, for the linear static case without body charge or forces, as [18, 19]

$$\mathcal{H}(\boldsymbol{\epsilon}, \boldsymbol{E}) = \iiint_V \left(\frac{1}{2} \epsilon_{ij} C^E_{ijmn} \epsilon_{mn} - \frac{1}{2} E_i k^{\epsilon}_{in} E_n + E_n e_{nij} \epsilon_{ij} \right) dV \tag{1}$$

In this equation, the independent variables are the elastic strain ϵ_{mn} and the electric field E_n. On the right side of the equation, C^E_{ijmn} are the elastic constitutive constants measured at constant electric field, e_{nij} are the piezoelectric constants (measured at a constant strain or electric field) and k^{ϵ}_{in} are the dielectric constants measured under constant strain. Differentiating this equation respect to the independent variables gives the constitutive equations of piezoelectricity as

$$\sigma_{ij} = \frac{\partial \mathcal{H}(\boldsymbol{\epsilon}, \boldsymbol{E})}{\partial \epsilon_{ij}} = C_{ijmn} \epsilon_{mn} + e_{nij} E_n \tag{2}$$

$$\text{and} \quad D_i = \frac{\partial \mathcal{H}(\boldsymbol{\epsilon}, \boldsymbol{E})}{\partial E_i} = e_{imn} \epsilon_{mn} - k_{in} E_n \tag{3}$$

where the stress is σ_{ij} and the electric displacement is D_i. The electrical field is related to the voltage through a gradient, equation (6), and the electrical field is related to the electrical displacement through equation (5):

$$\epsilon_{mn} = \frac{1}{2}(u_{m,n} + u_{n,m}) \tag{4}$$

$$D_m = k_{mn}\, E_n \tag{5}$$

$$\text{and} \quad E_m = -\phi_{,m} \tag{6}$$

From equation (2), in the linear case, the stress applied to a piezoelectric material is converted to elastic deformation and an electrical field proportional to the piezoelectric constitutive matrix. This electrical field will

also create a gradient through equation (6), which will generate the voltage from the energy harvester. Interestingly, this electrical field also provokes energy loss, since equations (3) and (5) shows that the electrical field will create a self-induced electrical field with opposite sign, proportional to the permittivity constants. Hence the voltage output from the energy harvester is maximized by reducing the permittivity constants and increasing the piezoelectric constants.

2.1 The Mori-Tanaka method

The porous piezoelectric material is composed by two phases; air and piezoelectric material. The piezoelectric material is normally lead zirconate titanate (PZT) or Barium Titanate. For each phase the material constants are well known, but the set of homogenized material constants must be calculated for the composite. One approach is to solve the detailed finite element model for specific percentages of random inclusions. However, this approach is computationally expensive, and requires many elements to obtain an accurate model. Moreover, for each percentage of material, the model must be re-calculated.

An alternative approach is to homogenize the material using analytical methods. One of the most well-known and validated approaches is the Mori-Tanaka method which is based on *mean-field homogenization theory*. This method improves the Eshelby solution [20] given for ellipsoidal inclusions in elastic mediums, and was expanded by Y. Benveniste [21] to include composite materials and later by M. L. Dunn and M. Taya [22] to electromechanical fields. The approach may be used in multi-field physics analysis, for example for general composite materials [23–26] and for porous piezoelectric materials [17]. To perform a Mori-Tanaka homogenization, the calculation of the Eshelby tensor is required. The procedure to obtain this tensor is comprehensively detailed in [27] and hence is not explained here.

In the Mori-Tanaka method, each inclusion with properties $\boldsymbol{E}^{\mathrm{I}}$, behaves as an isolated inclusion, embedded in an infinite matrix with properties $\boldsymbol{E}^{\mathrm{M}}$, that is loaded remotely by an applied strain. Hence each inclusion is subjected to the averaged stress fields acting on it from all of the other inclusions, through the superposition of stresses. The homogenization procedure of this method is briefly summarized. First an influence tensor has to be calculated for every phase r ($\boldsymbol{A}_0^{\mathrm{I},r}$) and percentage. This concentration tensor is assumed to be equal to the relation between the strain in the inclusion and the strain in the matrix [23]. Thus

$$\boldsymbol{E}^{\mathrm{I},r} = \boldsymbol{A}_0^{\mathrm{I},r}\ \boldsymbol{E}^{\mathrm{M}} \tag{7}$$

This concentration tensor is written in terms of the Eshelby tensor, $\boldsymbol{S}^*$, as

$$\boldsymbol{A}_0^{\mathrm{I},r} = \left[\boldsymbol{I} + \boldsymbol{S}^* \left(\boldsymbol{E}^{\mathrm{M}}\right)^{-1} \left(\boldsymbol{E}^{\mathrm{I},r} - \boldsymbol{E}^{\mathrm{M}}\right)\right]^{-1} \tag{8}$$

These concentration tensors are then averaged to obtain the general influence tensor, $\left(\boldsymbol{A}_{(\mathrm{MT})}^{\mathrm{I}}\right)$

$$\boldsymbol{A}_{(\mathrm{MT})}^{\mathrm{I},r} = \left[c^{\mathrm{I},r}\boldsymbol{I} + c^{\mathrm{M}}(\boldsymbol{A}_0^{\mathrm{I},r})^{-1} + \sum_{j=1}^{N} c^{\mathrm{I},r}\boldsymbol{A}_0^{\mathrm{I},j}(\boldsymbol{A}_0^{\mathrm{I},r})^{-1}\right]^{-1} \tag{9}$$

Finally, the effective electro-elastic material tensor ($\boldsymbol{E}^*$) is obtained using

$$\boldsymbol{E} = \sum_{r=1}^{N} c^r \boldsymbol{E}^r \boldsymbol{A}^r = \boldsymbol{E}^{\mathrm{M}} + \sum_{r=2}^{N} c^r \left(\boldsymbol{E}^{\mathrm{I}} - \boldsymbol{E}^{\mathrm{M}}\right) \boldsymbol{A}^r \tag{10}$$

and

$$\boldsymbol{E}_{(\mathrm{MT})}^* = \boldsymbol{E}^{\mathrm{M}} + \sum_{r=1}^{N} c^{\mathrm{I},r} \left(\boldsymbol{E}^{\mathrm{I},r} - \boldsymbol{E}^{\mathrm{M}}\right)\ \boldsymbol{A}^{\mathrm{I},r\ (\mathrm{MT})} \tag{11}$$

This method is self-consistent, since the inverse of the electromechanical matrix $\boldsymbol{E}^*$ is equal to the compliance electromechanical matrix $\boldsymbol{F}^*$.

2.2 Analytical Modelling of the Energy Harvester

The response of the energy harvester is predicted first by an analytical solution. A cantilever beam energy harvester is proposed; many authors have chosen this typology [1, 7, 8, 11, 12] due to the high strains developed at the clamped end, and because it is easy to build and test. Furthermore, analytical solutions for beam systems are highly developed, allowing representative models to be implemeted relatively easily. The proposed cantilever beam is composed of two piezoelectric layers with an elastic support layer in between, and clamped at the right side, as shown in fig. 1.

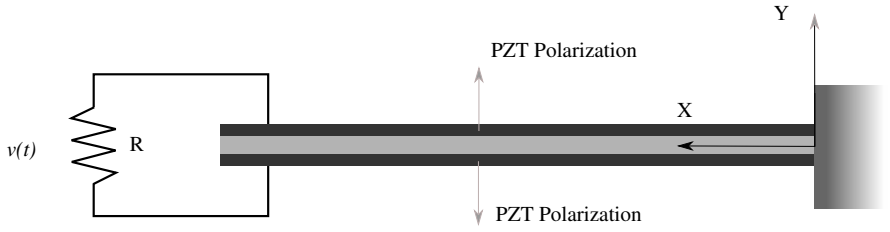

Figure 1: Schematic view of the cantilever beam energy harvester with the circuit configuration.

The beam is symmetric about its neautral axis, and its thickness is small compared to its length. An Euler-Bernoulli beam model is considered with a resistor connected in series to the electrodes on the top and bottom piezoelectric material surfaces. Following the approach presented in [2], the external circuit admittance, which is inversely proportional to the resistance, is related to the piezoelectric beam through the integral form of Gauss's law:

$$\frac{d}{dt}\left(\int_A \boldsymbol{D}\cdot\boldsymbol{n}\,dA\right) = \frac{v(t)}{R} \tag{12}$$

where R is the load resistance. Substituting equation (3) in equation (12), one obtains

$$\frac{k_{33}bL}{2h_p}\frac{dv(t)}{dt} + \frac{v(t)}{R} + e_{31}\frac{(h_p+h_e)}{2}b\int_0^L \frac{\partial^3 w(x,t)}{\partial x^2 \partial t}dx = 0 \tag{13}$$

In this equation, k_{33} is the permittivity coefficient and e_{31} is the piezoelectric coefficient. The geometrical dimensions b,L,h_p,h_e are the beam width, beam length, the piezoelectric layer thickness, and the elastic layer thickness. The displacement along the beam is represented by w; this is relative to the base motion of the cantilever beam. The voltage across the load resistor is $v(t)$. In equation (13) the unknown variables are $v(t)$ and the displacement w. Using a linear modal decomposition analysis, the displacements may be expanded as

$$w(x,t) = \sum_{n=1}^{\infty} \phi_n(x)\,\eta_n(t) \tag{14}$$

where $\phi_n(x)$ is the nth mass-normalized mode shape of the cantilever beam. The mechanical modal coordinate for the nth mode is η_n. Assuming a harmonic base excitation, the voltage is harmonic and given by $v(t) = V(\omega)\cdot e^{j\omega t}$. Then, from equations (13) and (14), the voltage $V(\omega)$ is [2]

$$V(\omega) = -\omega^2 W_0 \frac{\displaystyle\sum_{n=1}^{\infty} \frac{-j\omega\theta_n\sigma_n}{\omega_n^2 - \omega^2 + j2\zeta_n\omega_n\omega}}{\displaystyle\frac{1}{R} + j\omega C^{eq} + \sum_{n=1}^{\infty}\frac{j\omega\theta_n^2}{\omega_n^2 - \omega^2 + j2\zeta_n\omega_n\omega}} \tag{15}$$

where n is the mode number, ω is the frequency of the base excitation, w_n is the natural frequency of the n^{th} mode, W_0 is the amplitude of the base excitation, ζ_n is the modal damping for mode n, R is the load resistance of the device connected to the energy harvester, and j is the unit imaginary ($\sqrt{-1}$). The parameters σ_n, θ_n, C^{ep} are coefficients related to the inertia of the beam, the electro-mechanical coupling coefficient and the electrical capacitance respectively. For a cantilever beam without tip mass, and with the piezoelectric layers covering the whole length of the beam and connected in series, these coefficients are

$$\sigma_n = -m \int_0^L \phi_n(x) dx \tag{16}$$

$$\theta_n = e_{31} b \left(\frac{h_p + h_e}{2} \right) \left. \frac{d\phi_n}{dx} \right|_{x=L} \tag{17}$$

$$C^{eq} = \frac{k_{33}^S b L}{2 h_p} \tag{18}$$

where m is the mass per unit length of the beam.

The instantaneous power generated by the harvestor is obtained as $P = V \cdot I = V^2/R$, where I is the current through the resistor.

An analytical study is performed for harvesters with piezoelectric layers that have uniform properties, but for different percentages of inclusions. This will give some insight into the effect of porosity of the piezoelectric material on the energy harvester performance. Although the objective, namely to maximise the harvested power, is very clear, choosing the constraints to apply to the harvester system is not so straightforward. Hence three models will be considered, which show the effect of the percentage of piezoelectric material for a specific constraint (geometrical properties, mass and frequency). Unless otherwise specified, the geometrical properties in table 1 are used, and the material properties are given in equation (19). The three models are:

- *Model A. Thickness constant.* The geometry is constant, and only the percentage of inclusions in the piezoelectric material is varied.
- *Model B. Mass constant.* The mass of piezoelectric material remains constant. As the percentage of material in the piezoelectric layers decreases, the thickness increases at the same rate to keep the piezoelectric material mass constant.
- *Model C. The first mechanical natural frequency is kept constant.* The mass and stiffness of the beam is changed by the percentage of the piezoelectric material, and hence the first natural frequency is also changed. The thickness is modified by an iterative solver to fix the first natural frequency (to 185Hz in the example).

2.3 Finite Element Modelling

In this section the finite element model (FEM) used is explained briefly. The FEM may be used to validate the beam model, but will also allow the distribution of piezoelectric material to be optimized by varying the porosity along the length and through the thickness of the beam. The model uses Matlab ® to launch the FEM model code in ANSYS®. The model uses 2D elements to reduce the computational cost, and the element type used for the piezoelectric material is PLANE223. This element has 8 nodes and a quadratic displacement behavior. For the non-piezoelectric elements, the element type is PLANE183, which also has 8 nodes and a quadratic displacement behavior. The FE model is coded using the APDL programming language, a proprietary language used in ANSYS®.

The user chooses the percentage at a reduced number of sections of the beam; the Matlab® script then interpolates these values to give a fine distribution, using a cubic spline with zero slope at the beginning

and end of the beam. This distribution is discretized into elements with constant properties given at their central point. The nodes, element and material properties are then written to input files for ANSYS®. After ANSYS® has solved the model, the APDL code prints the results to different output files which are read by the Matlab® script.

3 Results

The geometrical properties of the cantilever beam and the material properties of the elastic support, are detailed in table 1. The material used in the simulations is PZT-5A, whose properties are given by [2]

Geometry		**Elastic Material Properties**	
Beam Length (mm)	30	Elastic Modulus (GPa)	70
Piezoelectric Thickness (mm)	0.15	Poisson's ratio	0.3
Elastic Layer Thickness (mm)	0.05		
Analysis Parameters			
Modal Damping Ratios	0.01, 0.012, 0.03, 0.059, 0.097		
Load Resistance (Ω)	10, 100, 100, 1000, 10000, 100000, 1000000, 10000000, 100000000		

Table 1: Geometrical properties of the beam, material properties of the elastic support material and analysis parameters.

$$
\boldsymbol{E}^{\mathrm{M}} = \left(\begin{array}{cccccc|ccc}
121 & 75.4 & 75.2 & 0 & 0 & 0 & 0 & 0 & 5.4 \\
 & 121 & 75.2 & 0 & 0 & 0 & 0 & 0 & 5.4 \\
 & & 111 & 0 & 0 & 0 & 0 & 0 & -15.8 \\
 & & & 21.1 & 0 & 0 & 0 & -12.3 & 0 \\
 & \multicolumn{2}{c}{Symmetric} & & 21.1 & 0 & -12.3 & 0 & 0 \\
 & & & & & 22.9 & 0 & 0 & 0 \\
\hline
0 & 0 & 0 & 0 & 12.3 & & 919 & 0 & 0 \\
0 & 0 & 0 & 12.3 & 0 & 0 & & 919 & 0 \\
-5.4 & -5.4 & 15.8 & 0 & 0 & 0 & Symm. & & 826.6
\end{array}\right)
$$

$$
\text{Units} = \left(\begin{array}{c|c}
\boldsymbol{C}\ (\mathrm{GPa}) & \boldsymbol{e}^T\ (\mathrm{C/m^2}) \\
\hline
\boldsymbol{e}\ (\mathrm{C/m^2}) & \boldsymbol{k}_T/k_0
\end{array}\right) \qquad \begin{array}{l} \text{Density} = 7750\ \mathrm{kg/m^3} \\ k_0 = 8.854 \cdot 10^{-12}\ \mathrm{pF/m} \end{array} \tag{19}
$$

At an initial step, the homogenized material properties are obtained using the Mori-Tanaka method. The resulting homogenized properties of the porous material for 50% to 100% of piezoelectrical material are shown in fig. 2. This method gives smooth and consistent results, close to the results given in [17].

The dynamic behavior of different beam models with different levels of of porosity is analyzed for harmonic base excitation with an amplitude of 1 mm and in the frequency range of 1Hz to 10kHz. The frequency response for model A, which has constant percentage of inclusions along the length, is shown in fig. 3 . Under 40% of matrix (piezoelectric) material, the porous structure is not stable due to cracks and the lack of a consistent structure [13]; hence, the percentages analyzed are between 50% and 100%. The effect of the porosity is to reduce the resonance frequency, and also to reduce the maximum displacement.

The reduced displacement will lead to a reduced output voltage. This is shown in fig. 4, which gives the voltage FRF for a range of frequencies close to the first mode for different constant percentages of PZT. The shift in the resonance frequencies is about 30Hz and the reduction in voltage between the non-porous case and the 50% porous case is about 42.7%.

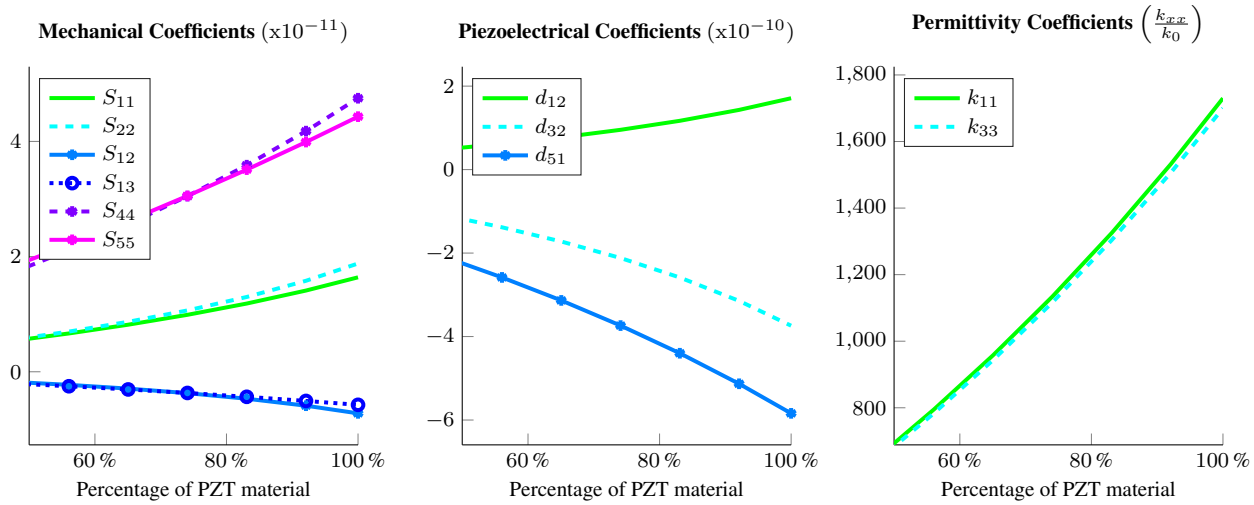

Figure 2: The estimated material coefficients obtained using the Mori-Tanaka method.

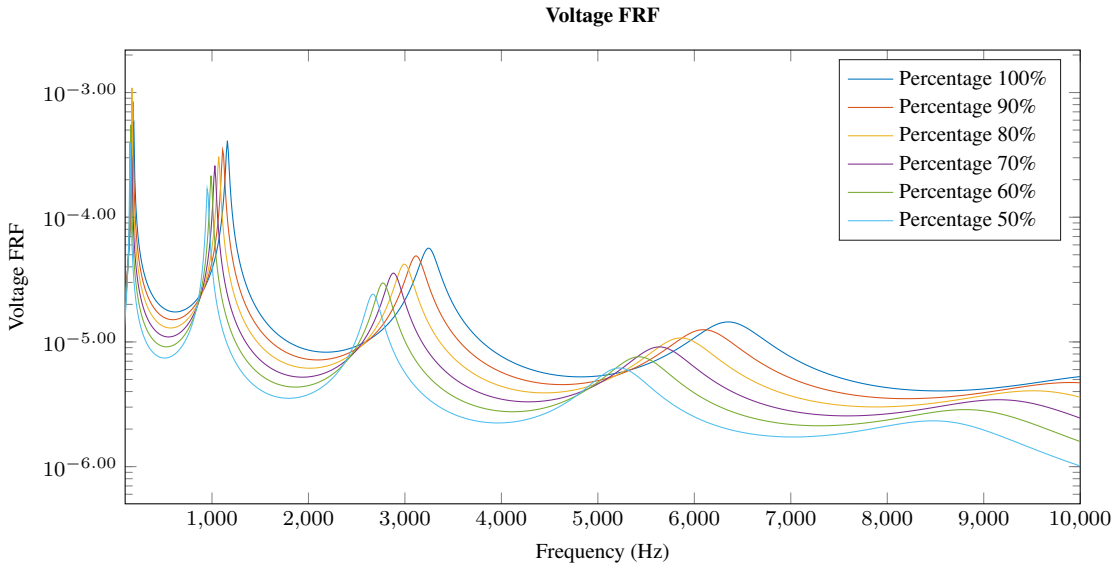

Figure 3: Frequency response for different percentages of piezoelectric material.

The results for the different simulated models are shown in figs. 5, 6 and 7. Three results are shown as surfaces. The first is the maximum voltage near the first mode as a function of load resistance and piezoelectric material percentage. The second is the maximum power harvested around the first mode. The third gives the frequency where this maximum power is achieved.

The results for *Model A* are shown in figures 5(a), 5(b) and 5(c). The voltage generated by the energy harvester decreases smoothly with the percentage of piezoelectric material. The reduction in the quantity of the PZT material leads to a reduction in all of the main parameters, namely frequency, voltage and power.

The results for *Model B* are shown in figure 6(a), 6(b) and 6(c). This model keeps the mass of the piezoelectric material constant as the percentage of piezoelectric material varies. Hence, to keep the mass constant, the thickness of the piezoelectric layers have to be increased in the same ratio to the porosity increase. The results show a significant increase in the voltage generated, as well as the power harvested. Interestingly, the resonance frequency in these cases tends to increase as the the porosity increases. This trend is in contrast to that shown by the model A, and is due to the increasing thickness of the harvester, which moves piezoelectric material further from the neutral axis, hence increases the strain in the piezoelectric layer. Higher strains in the piezoelectric layers, contribute to an increase in the electrical field generated by the piezoelectric effect,

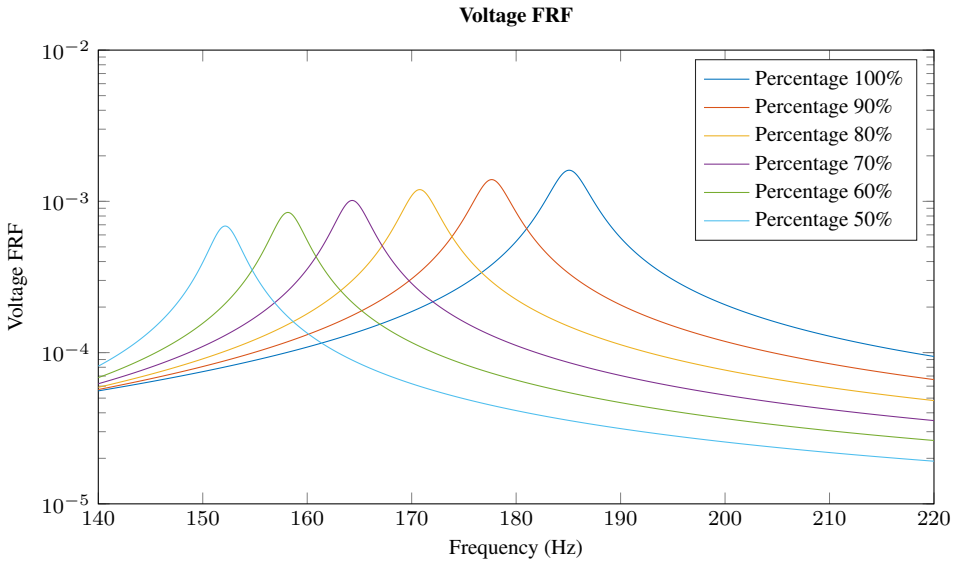

Figure 4: The voltage frequency response around the first mode for different percentages of piezoelectric material.

and therefore the voltage. The increasing frequency means that the stiffness variation is lower than the mass variation, due to the non-linear variation in the electromechanical properties calculated by the Mori-Tanaka method. In contrast, the mass changes linearly with the percentage of piezoelectric material, and has a bigger impact on the resonance frequency.

The results for *Model C* are shown in figures 7(a), 7(b) and 7(c). The first mechanical natural frequency of the energy harvester is fixed at 185Hz. To obtain this frequency, the thickness of the piezoelectric layer is varied. The trends for this model are quite similar to the ones obtained for *Model A*, with decreasing frequency, voltage and frequency for increasing porous inclusion percentage.

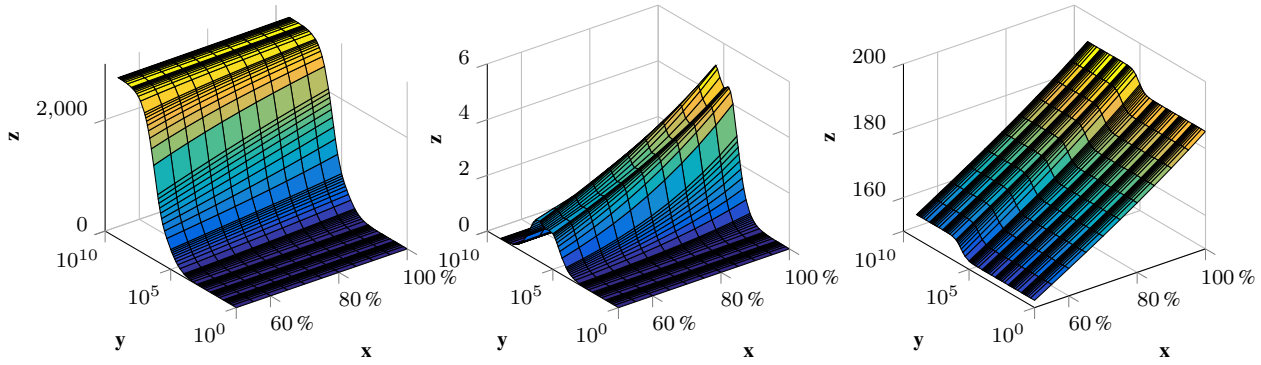

(a) Voltage (b) Power (c) Frequency

Figure 5: Results for *Model A: Thickness constant*. The x-axis is the percentage piezoelectric material and y-axis is the load resistance: (a) the maximum voltage of the energy harvester under harmonic excitation for frequencies around the first resonance; (b) The maximum power around the first resonance; (c) the frequency for maximum power.

4 Conclusions

The dynamic behaviour of a porous piezoelectric energy harvester was analysed. The dynamic response has been predicted using an analytical model of a simple bimorph cantilever beam. The modeling process

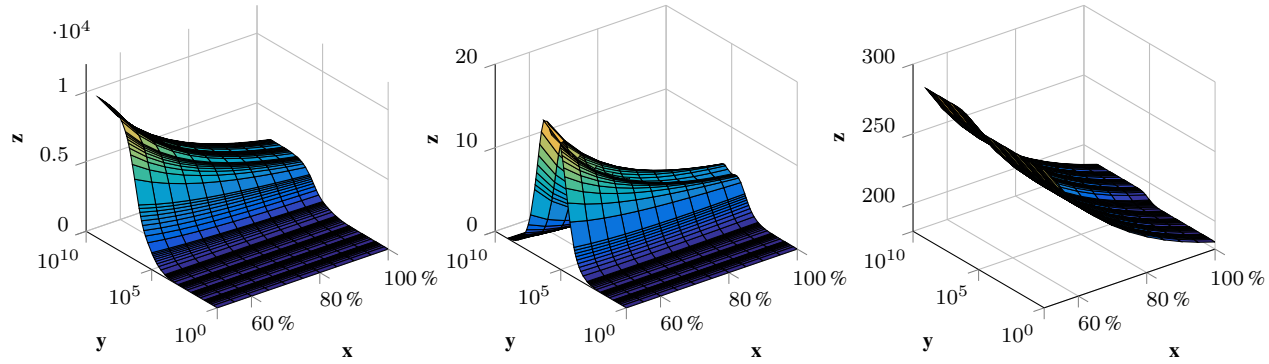

(a) Voltage (b) Power (c) Frequency

Figure 6: Results for *Model B: Mass constant*. The x-axis is the percentage piezoelectric material and y-axis is the load resistance: (a) the maximum voltage of the energy harvester under harmonic excitation for frequencies around the first resonance; (b) The maximum power around the first resonance; (c) the frequency for maximum power.

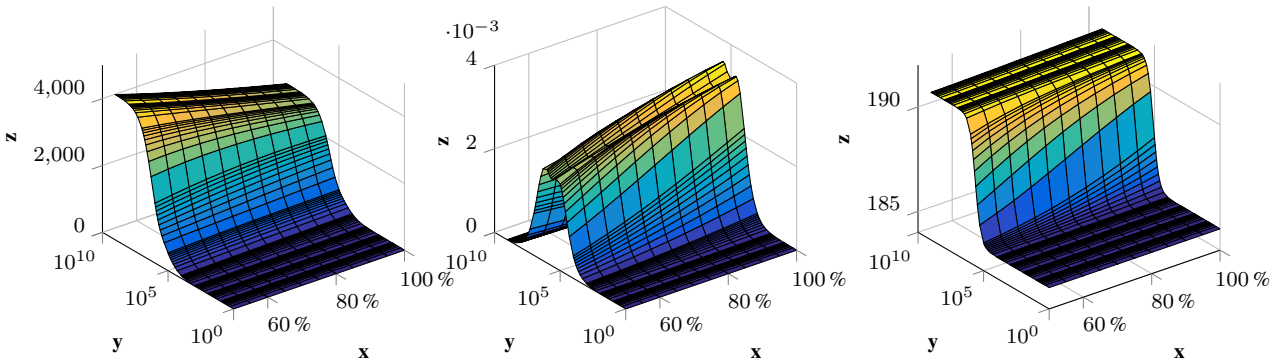

(a) Voltage (b) Power (c) Frequency

Figure 7: Results for *Model C: Frequency constant*. The x-axis is the percentage piezoelectric material and y-axis is the load resistance: (a) the maximum voltage of the energy harvester under harmonic excitation for frequencies around the first resonance; (b) The maximum power around the first resonance; (c) the frequency for maximum power.

requires a homogenization approach, which in this case have been performed using the Mori-Tanaka method. The results shows a general decrease of the material properties and energy harvested by the device with a decrease in the mass of the piezoelectric material. When the mass of the piezoelectric material is fixed for each level of porosity (*Model B*) the results shows a significant improvement in the energy harvested. These results show that using porous material to optimize the distribution of piezoelectric material can harvest more energy than a non-porous material. The present paper is part of ongoing research at Swansea University investigating the applications of porous materials for energy harvesting. In future research the impact of the distribution of the porosity along the thickness and length will be studied using the FE model presented.

Acknowledgements

The authors acknowledge the financial support from the Sêr Cymru National Research Network and Swansea University through a Postgraduate Scholarship.

References

[1] A. Erturk, D. J. Inman. *An experimentally validated bimorph cantilever model for piezoelectric energy harvesting from base excitations*. Smart Materials and Structures, vol. 18, no. 2 (2009), p. 025009.

[2] A. Erturk, D. J. Inman. *Piezoelectric energy harvesting*. John Wiley & Sons (2011). ISBN 9781119991151.

[3] A. Erturk, D. J. Inman. *On mechanical modeling of cantilevered piezoelectric vibration energy harvesters*. Journal of Intelligent Material Systems and Structures (2008).

[4] H. A. Sodano, D. J. Inman, G. Park. *A review of power harvesting from vibration using piezoelectric materials*. Shock and Vibration Digest, vol. 36, no. 3 (2004), pp. 197–206.

[5] H. A. Sodano, D. J. Inman, G. Park. *Comparison of piezoelectric energy harvesting devices for recharging batteries*. Journal of Intelligent Material Systems and Structures, vol. 16, no. 10 (2005), pp. 799–807.

[6] S. R. Anton, H. A. Sodano. *A review of power harvesting using piezoelectric materials (2003–2006)*. Smart Materials and Structures, vol. 16, no. 3 (2007), p. R1.

[7] M. I. Friswell, S. F. Ali, O. Bilgen, S. Adhikari, A. W. Lees, G. Litak. *Non-linear piezoelectric vibration energy harvesting from a vertical cantilever beam with tip mass*. Journal of Intelligent Material Systems and Structures, vol. 23, no. 13 (2012), pp. 1505–1521.

[8] S. Adhikari, M. I. Friswell, D. J. Inman. *Piezoelectric energy harvesting from broadband random vibrations*. Smart Materials and Structures, vol. 18, no. 11 (2009), p. 115005.

[9] C. J. Rupp, A. Evgrafov, K. Maute, M. L. Dunn. *Design of piezoelectric energy harvesting systems: a topology optimization approach based on multilayer plates and shells*. Journal of Intelligent Material Systems and Structures, vol. 20, no. 16 (2009), pp. 1923–1939.

[10] V. R. Challa, M. Prasad, Y. Shi, F. T. Fisher. *A vibration energy harvesting device with bidirectional resonance frequency tunability*. Smart Materials and Structures, vol. 17, no. 1 (2008), p. 015035.

[11] E. Lefeuvre, D. Audigier, C. Richard, D. Guyomar. *Buck-boost converter for sensorless power optimization of piezoelectric energy harvester*. Power Electronics, IEEE Transactions on, vol. 22, no. 5 (2007), pp. 2018–2025.

[12] G. K. Ottman, H. F. Hofmann, A. C. Bhatt, G. A. Lesieutre. *Adaptive piezoelectric energy harvesting circuit for wireless remote power supply*. Power Electronics, IEEE Transactions on, vol. 17, no. 5 (2002), pp. 669–676.

[13] C. R. Bowen, A. Perry, A. Lewis, H. Kara. *Processing and properties of porous piezoelectric materials with high hydrostatic figures of merit*. Journal of the European Ceramic Society, vol. 24, no. 2 (2004), pp. 541–545.

[14] J. F. Li, K. Takagi, M. Ono, W. Pan, R. Watanabe, A. Almajid, M. Taya. *Fabrication and evaluation of porous piezoelectric ceramics and porosity–graded piezoelectric actuators*. Journal of the American Ceramic Society, vol. 86, no. 7 (2003), pp. 1094–1098.

[15] E. Roncari, C. Galassi, F. Craciun, C. Capiani, A. Piancastelli. *A microstructural study of porous piezoelectric ceramics obtained by different methods*. Journal of the European Ceramic Society, vol. 21, no. 3 (2001), pp. 409–417.

[16] J. I. Roscow, J. Taylor, C. R. Bowen. *Manufacture and characterization of porous ferroelectrics for piezoelectric energy harvesting applications*. Ferroelectrics, vol. 498, no. 1 (2016), pp. 40–46.

[17] M. L. Dunn, M. Taya. *Electromechanical properties of porous piezoelectric ceramics*. Journal of the American Ceramic Society, vol. 76, no. 7 (1993), pp. 1697–1706.

[18] Q. Qin. *Advanced mechanics of piezoelectricity*. Springer Science & Business Media (2012).

[19] E. P. Eer Nisse. *Variational method for eletcroelasticvibration analysis*. The Journal of the Acoustical Society of America, vol. 40, no. 5 (1966), pp. 1260–1260.

[20] J. D. Eshelby. *The determination of the elastic field of an ellipsoidal inclusion, and related problems*. In *Proceedings of the Royal Society of London A: Mathematical, Physical and Engineering Sciences*, vol. 241. The Royal Society (1957), pp. 376–396.

[21] Y. Benveniste. *A new approach to the application of mori-tanaka's theory in composite materials*. Mechanics of materials, vol. 6, no. 2 (1987), pp. 147–157.

[22] M. L. Dunn, M. Taya. *An analysis of piezoelectric composite materials containing ellipsoidal inhomogeneities*. In *Proceedings of the Royal Society of London A: Mathematical, Physical and Engineering Sciences*, vol. 443. The Royal Society (1993), pp. 265–287.

[23] B. Klusemann, B. Svendsen. *Homogenization methods for multi-phase elastic composites: Comparisons and benchmarks*. Technische Mechanik, vol. 30, no. 4 (2010), pp. 374–386.

[24] S. Kurukuri, S. Eckardt. *A review of homogenization techniques for heterogeneous materials*. Advanced Mechanics of Materials and Structures, Graduate School in Structural Engineering, Germany (2004).

[25] O. Pierard, C. Friebel, I. Doghri. *Mean-field homogenization of multi-phase thermo-elastic composites: a general framework and its validation*. Composites Science and Technology, vol. 64, no. 10 (2004), pp. 1587–1603.

[26] T. Te Wu. *The effect of inclusion shape on the elastic moduli of a two-phase material*. International Journal of Solids and Structures, vol. 2, no. 1 (1966), pp. 1–8.

[27] Y. Mikata. *Determination of piezoelectric eshelby tensor in transversely isotropic piezoelectric solids*. International Journal of Engineering Science, vol. 38, no. 6 (2000), pp. 605–641.